THE JOURNAL OF PHYSICAL CHEMISTRY Letters

Letter

Cite This: J. Phys. Chem. Lett. 2018, 9, 6656−6661

pubs.acs.org/JPCL

Phonon-Assisted Photoluminescence Up-Conversion of Silicon-Vacancy Centers in Diamond

Yuan-Fei Gao,[†,‡] Qing-Hai Tan,[‡] Xue-Lu Liu,[‡] Shu-Liang Ren,[‡] Yu-Jia Sun,[‡] Da Meng,[‡] Ying-Jie Lu,[†] Ping-Heng Tan,[‡,§] Chong-Xin Shan,*[,†] and Jun Zhang*[,‡,§]

[†]Henan Key Laboratory of Diamond Optoelectronic Materials and Devices, School of Physics and Engineering, Zhengzhou University, Zhengzhou 450052, People's Republic of China

[‡]State Key Laboratory of Superlattices and Microstructures, Institute of Semiconductors, Chinese Academy of Sciences, & College of Materials Science and Optoelectronic Technology, University of Chinese Academy of Sciences, Beijing 100083, People's Republic of China

[§]CAS Center of Excellence in Topological Quantum Computation, University of Chinese Academy of Sciences, Beijing 101408, People's Republic of China

ABSTRACT: Phonon-assisted anti-Stokes photoluminescence (ASPL) up-conversion lies at the heart of optical refrigeration in solids. The thermal energy contained in the lattice vibrations is taken away by the emitted anti-Stokes photons' ASPL process, resulting in laser cooling of solids. To date, net laser cooling of solids is limited in rare-earth (RE)-doped crystals, glasses, and direct band gap semiconductors. Searching more solid materials with efficient phonon-assisted photoluminescence up-conversion is important to enrich optical refrigeration research. Here, we demonstrate the phonon-assisted PL up-conversion process from the silicon vacancy (SiV) center in diamond for the first time by studying ASPL spectra for the dependence of temperature, laser power, and excitation energy. Although net cooling has not been observed, our results show that net laser cooling might be eventually achieved in diamond by improving the external quantum efficiency to higher than 95%. Our work provides a promising route to investigate the laser cooling effect in diamond.

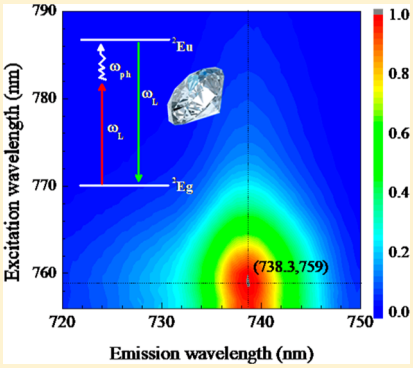

Optical refrigeration or laser cooling in solids based on anti-Stokes photoluminescence (ASPL) was first proposed by Peter Pringsheim as early as 1929.[1] Because the thermal energy in solids is primarily stored in the quanta of the atomic vibrational degrees of freedom, i.e., phonons, the optical refrigeration relies on continual annihilation of the phonons during a phonon-assisted PL up-conversion process. This proposal initially stimulated a debate as it was believed to contradict the second law of thermodynamics. This controversy was reconciled when Landau formally introduced entropy to optical radiation (i.e., light) to explain Pringsheim's ideas in 1946.[2] Laser cooling of solids exhibits advantages of compactness, being free of vibration and cryogen, as well as high reliability,[3−5] which show a wide range of potential applications in military, surveillance, security, aerospace, fundamental research, and commercial applications such as infrared cameras, space-based imagers, γ-ray spectrometers, precision metrology, and cryoelectron tomography.[3,4,6−8] To realize net laser cooling of solids, the material must have high external quantum efficiency, efficient phonon-assisted PL up-conversion, as well as large spectral overlap between the emission and absorption cross sections.[4,5,9] Under these special constraints, the materials suitable for laser cooling to date are limited to rare-earth (RE)-doped glasses or crystals and direct band gap semiconductors.[5,9−13]

Diamond is a wide-band semiconductor (5.47 eV at room temperature) with a moderate refractive index of 2.4 and is optically transparent from the deep-ultraviolet to infrared spectra region. Moreover, diamond is an excellent thermal conductor (2×10^3 W m^{-1} K^{-1}) that exhibits low thermal expansion, high breakdown voltage, and high carrier mobility.[14] With proper engineering and optimization, diamond can be a potentially attractive candidate for electronic, optical, and thermal applications. Furthermore, diamond is biocompatible and chemically robust. Recent advances in the perfection of diamonds have been dramatic. Arguably more interesting is the precise control and application of diamond's color centers, which can be harnessed for quantum, sensing, and labeling applications.[15] Spin properties of diamond defects also have attracted much attention owing to their long spin coherence times. Because spin time usually increases at low temperatures, a new way of cooling diamond is important for quantum information and quantum sensing where long spin relaxation times are needed. Recently, a theoretical investigation of the capability of optical refrigeration used diamond[16] and, in particular, nitrogen

Received: September 17, 2018
Accepted: October 24, 2018
Published: October 24, 2018

DOI: 10.1021/acs.jpclett.8b02862
J. Phys. Chem. Lett. 2018, 9, 6656−6661

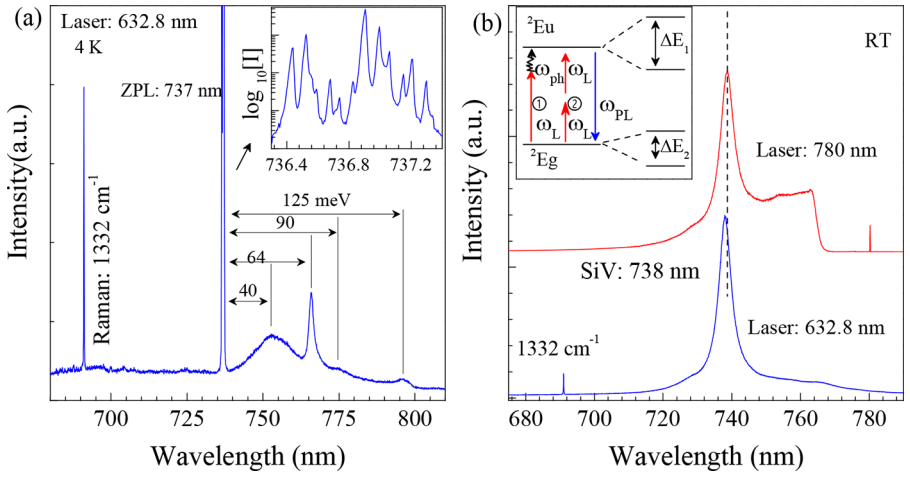

Figure 1. PL and ASPL of the SiV center in diamond at low and room temperature. (a) PL spectra of the SiV center excited by 632.8 nm with an average power of 4 mW at 4 K. The peak at 1332 cm^{-1} is the first-order Raman spectrum of the optical phonon in the Brillioun zone center of diamond. The ZPL and its phonon replica are identified. The fine structures of ZPL are shown in the inset. (b) Stokes PL (blue) and ASPL (red) spectra excited by 632.8 and 780 nm at room temperature, respectively. (Inset) Photon up-conversion processes between ground and excited states of the SiV center: (1) phonon-assisted PL up-conversion process by absorbing one photon and phonon energy, (2) two-photon PL up-conversion process by absorbing two photons.

vacancy (NV) or silicon vacancy (SiV) defects in diamond. They predict that cooling can be achieved by using both defects due to its high quantum efficiency. Owing to the large band gap of diamond, emission from such color centers can escape the crystal without absorption and lead to a high external quantum efficiency, which can be improved further by optimizing the parameters of diamond growth, with special cutting techniques, and coupling with high-quality factor microcavities.[17] Besides high external quantum efficiency, spectral overlap between the emission and absorption cross sections determines the possible cooling zone, where only the pump laser energy inside can achieve the ASPL process and thus a possible net cooling.[16,18−20] Comparing with NV centers, SiV centers are more suitable for laser cooling due to their narrow emission spectrum and significant spectral overlap between the emission and absorption cross sections.[16] Therefore, we may expect SiV centers to exhibit a greater cooling capability. Furthermore, through careful materials engineering, it is possible to achieve >80% conversion of implanted silicon to SiV.[17] Its optical properties are very favorable, with ∼90% of its emission into the zero-phonon line (ZPL) and near-transform-limited optical line widths.

Phonon-assisted ASPL is the first requirement to realize the possibility and can influence the performance of laser cooling. In this letter, we experimentally investigate the phonon-assisted ASPL of SiV in diamond crystals for the first time. By analyzing their ASPL on the dependence of temperature, pump power, and excitation energy, we confirm that phonon-assisted ASPL exists in the SiV centers and obtain the best red-detuning energy of cooling pumping of around 50 meV at room temperature.

The Stokes PL and ASPL spectra of the SiV defects excited by 632.8 and 780 nm lasers were measured at 4 K and room temperature, respectively. As shown in Figure 1a, several optical peaks are clearly observed. The very sharp Raman peak at 1332 cm^{-1} is from a zone-center optical phonon with $\Gamma^{(2S+)}$ (F_{2g}) symmetry in diamond, meaning good crystalline quality.[21] The peak at around 737 nm is from the ZPL of SiV centers, which shows a 12-line fine structure, as shown in the inset of Figure 1a. The 12-line ZPLs can be divided into three subgroups that contributed from naturally occurring ^{28}Si, ^{29}Si, and ^{30}Si isotopes, where each Si isotope contributes four lines due to state transition from one of two ground states split by 0.02 meV to a doublet excited state split by 1.07 meV.[22] The ZPL−phonon coupling leads to a phonon replica of the ZPL. Depending on the phonon energy interacted with the ZPL, we identify those phonon replicas as a local-mode (40 meV) replica (756 nm), TA-mode (64 meV) replica (767 nm), local-mode (90 meV) replica (778 nm), and LA-mode (125 meV) replica (797 nm).[23] The strong intensities of phonon replicas indicate the strong electron−phonon coupling in SiV states. As the temperature increases, the line widths of the ZPL fine structures broaden and their peak energies gradually red shift; in addition, all spectra merge into one broad peak centered at 739 nm at room temperature, as shown in Figure 1b.

When we shift the pump laser to the lower-energy side of the SiV emission, the ASPL of ZPL and its replica of the SiV center can be observed, as shown in Figure 1b (red solid line). Compared with the Stokes PL spectrum (blue solid line) excited by 632.8 nm, the phonon replica in ASPL (red solid line) shows a much higher intensity due to the possible phonon-assisted ASPL process where the smaller energy difference between the emission and pumping laser should have higher transition possibility of phonon-assisted ASPL.[4,5,19] As shown in the inset of Figure 1b, there are two mechanisms to achieve the PL up-conversions.[5,18,19] One process is phonon-assisted ASPL by absorbing one phonon. During this process, the phonons, i.e., the thermal energy of the lattice, are removed and the sample is cooled. Following the phonon-assisted process, there are two distinguishing properties for the phonon-assisted ASPL: (1) the ASPL intensity is linearly dependent on the pumping laser power due to the single-photon absorption process; (2) the temperature dependence of ASPL should be proportional to the product of Bose−Einstein statistical functions of phonons $[\exp(\Delta E/k_BT) - 1]^{-1}$ and the external quantum efficiency of luminescence $\eta_{exe}(T)$ because the ASPL intensity is determined by the phonon population and recombination rate of electron−hole

DOI: 10.1021/acs.jpclett.8b02862
J. Phys. Chem. Lett. 2018, 9, 6656−6661

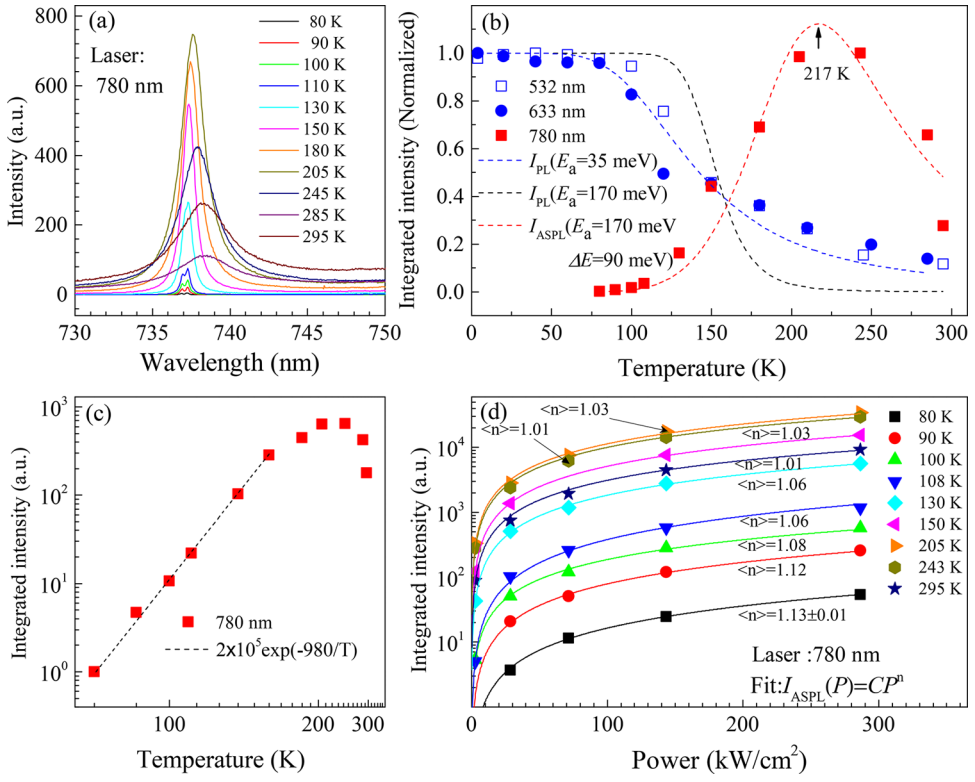

Figure 2. Temperature and laser power dependence of Stokes PL and ASPL. (a) ASPL spectra excited by a 780 nm laser with a power of 137 kW/cm^2 at different temperatures. (b) Temperature dependences of integrated densities of Stokes and anti-Stokes ZPL peaks excited by 532, 632.8, and 780 nm. Each curve is normalized by its highest value. The dashed curves are the fitting results by using the Stokes PL mode and ASPL mode. The fitting parameters E_a and ΔE are noted. (c) ASPL intensity ratio depending on the temperature in a logarithmic−reciprocal coordinate, where the vertical coordinate is logarithmic scale and the horizontal coordinate is reciprocal scale. The black dashed line is an exponential fitting using the function $R = I(T)/I(80\ \mathrm{K}) = 2 \times 10^5 e^{-980/T}$. (d) Integrated intensity of ASPL as a function of the 780 nm laser power measured at different temperatures. The experiment data is fitted by $I_{ASPL}(P) = CP^n$, where I_{ASPL} is the integrated intensity of ASPL, P is the laser power density, n is the power index, and C is a fitting constant.

pairs.[4,5,24] Another up-conversion mechanism is the two-photon PL process by absorbing two photons simultaneously, and the two-photon ASPL intensities are proportional to the $\eta_{exe}(T)$ and quadratically depend on the laser power.[4,5,24] In conclusion, by investigating the temperature dependence of ASPL, we can easily identify whether the phonon-assisted ASPL up-conversion dominates or not. Then, by checking the pumping power dependence, we can analyze the contribution of two-photon absorption and evaluate the pumping power range for the phonon-assisted process because two-photon absorption always happens in semiconductors if the laser power is high enough.

First, we measured the temperature dependence of Stokes PL and ASPL excited by blue-detuned and red-detuned lasers. Figure 2a shows the temperature dependence of the ASPL spectra excited by a 780 nm laser. Figure 2b shows the temperature dependences of the integrated intensities of Stokes PL spectra excited by 532 and 632.8 nm, as well as the ASPL spectra excited by 780 nm. The ASPL intensity increases quickly with temperature increasing from 80 to 217 K. When the temperature increases from 217 to 300 K, the ASPL intensity decreases gradually. Differently, for the Stokes PL excited by either 632.8 or 532 nm, both of their intensities are almost a constant from 4 to 100 K and then nonlinearly decrease with temperature increasing from 100 to 300 K. As we discussed previously, the Stokes PL intensity is mainly dominated by the external quantum efficiency of luminescence. The external quantum efficiency is determined by the radiative recombination rate W_r, nonradiative recombination rate W_{nr}, as well as the luminescence escape efficiency η_e:$\eta_{exe}(T) = \eta_e W_r/(\eta_e W_r + W_{nr})$, where $W_r = \alpha T^{-3/2}$, $W_{nr} = \beta e^{-E_a/k_B T}$, and η_e is a temperature-independent constant, and thus, we suppose η_e = 1 for simplicity.[5,9] Then we can derive the temperature dependence of the Stokes PL intensity as $I_{PL}(T) = I_0 \alpha T^{-3/2}/(\alpha T^{-3/2} + \beta e^{-E_a/k_B T})$, where E_a represents the thermal activation energy for the nonradiative process, k_B is the Boltzmann constant, and I_0, α, and β are the fitting parameters. For the phonon-assisted ASPL process, the intensity of ASPL is proportional to the product of the external quantum efficiency η_{exe} and phonon population. Thus, the temperature dependence of the phonon-assisted ASPL intensity can be written as $I_{ASPL}(T) = I_0 \alpha T^{-3/2}(\alpha T^{-3/2} + \beta e^{-E_a/k_B T})^{-1}[e^{\Delta E/k_B T} - 1]^{-1}$, where ΔE is the up-conversion energy, defined as the energy difference between the mean energy of luminescence and pump laser energy.

Below 100 K, η_{exe} is almost a constant, and the intensity of Stokes PL becomes nearly independent of temperature. At high temperature, the nonradiative recombination dominates, resulting in an exponential decay of the emission intensity. By using the formula $I_{PL}(T)$ above, we fit the experimental data as shown in Figure 2b with the dashed curve. The fitting curve is strongly dependent on the activation energy of the SiV center, which varies depending on the sample properties and has been reported as 16 meV in stabilization of the SiV by deliberate

DOI: 10.1021/acs.jpclett.8b02862
J. Phys. Chem. Lett. 2018, 9, 6656−6661

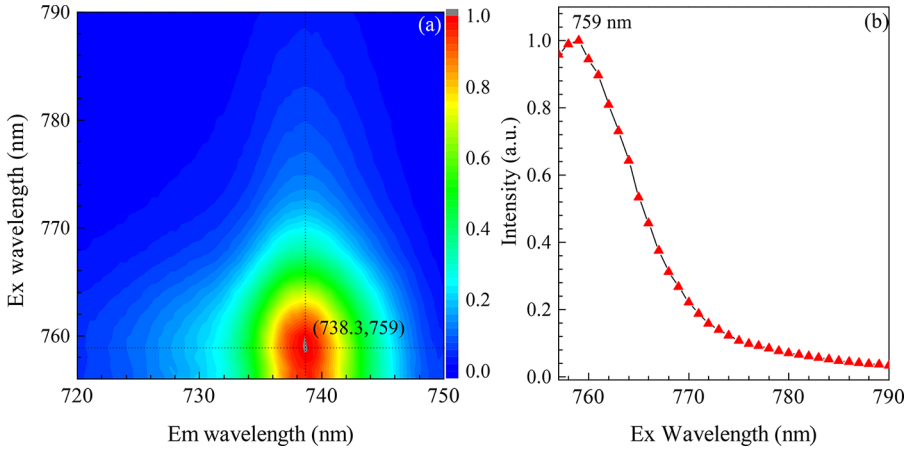

Figure 3. Anti-Stokes PLE spectra of ZPL at room temperature. (a) Contour plot of PLE spectra. The vertical axis represents the excitation (Ex) wavelength, while the horizontal axis is the emission (Em) wavelength. The color scales the ASPL intensity. (b) Normalized intensity of the ZPL (738 nm) dependent on the excitation wavelengths.

engineering of the diamond host,[17] 70 meV in polycrystalline diamond samples,[23] and 180 meV in ion-implanted single-crystal diamond.[25] In our case, we found that E_a = 35 meV gives a perfect fitting for Stokes PL excited by both 532 and 633 nm. For the ASPL process, we found that the phonon-assisted ASPL model $I_{ASPL}(T)$ gives the best fitting, where we obtain E_a = 170 meV and the up-conversion energy for ZPL is ΔE = 90 meV at 780 nm pumping (the ZPL peak is 739 nm). For comparison, we also plot the $I_{PL}(T)$ with E_a = 170 meV, where we can see that the trend of fitting is correct but with a much steeper transition at larger activation energy. The fitting result means that the ASPL pumped by 780 nm is a phonon-assisted up-conversion process. Generally, the phonon-assisted ASPL intensity is a competing result between the external quantum efficiency and phonon-assisted up-conversion efficiency. Below 217 K, the phonon-assisted up-conversion efficiency determines the intensity of ASPL, and thus, it shows an experiential increase with temperature increasing from 80 to 217 K. Above 217 K, although the phonon population is increasing, the nonradiative recombination rate increases much faster; thus, the external quantum efficiency of luminescence is dramatically decreased. As a result, the temperature dependence of the ASPL intensity is dominated by η_{exe} and shows a decreasing trend above 217 K. In Figure 2c, we plot the ASPL intensity ratio depending on the temperature in a logarithmic−reciprocal coordinate. We can see that the intensity of ASPL shows perfect exponential growth behavior. It hints that the intensity ratio of ASPL should be a very sensitive noncontact technique to measure the relative temperature change of the sample. By using a simple exponential function $R = I(T)/I(80\ \mathrm{K}) = 2 \times 10^5 e^{-980/T}$, we obtain a perfect fitting from 80 to 150 K. We can use this function to easily obtain the sample temperature once we obtain the intensity ratio R.

Pumping power is another important parameter for cooling experiments. Usually, we hope that the pump laser power is as high as possible to get the best cooling performance.[5,11] However, the two-photon absorption-induced ASPL emerges and dominates the up-conversion process if the laser power is too high, which will contribute to the heating effect and suppress the cooling process. For example, in laser cooling of CdS,[5] two-photon absorption dominates the ASPL process when the laser power density is higher than 0.3 MW/cm^2. The two-photon-induced ASPL usually shows a significant contribution when the sample defect density is very high, where the power dependence of ASPL in CdS shows a $P^{1.6}$ or $P^{1.4}$ contribution, and the cooling effect is totally suppressed by two-photon-induced heating.[26,27] In Figure 2d, we show the laser power dependence of ASPL excited by a 780 nm laser at different temperatures. The fittings of CP^n show that the mean power index $\langle n \rangle$ is almost equal to 1 above 90 K. Below 90 K, the two-photon absorption emerges and shows a $\langle n \rangle$ = 1.12 and 1.13 because of the low-phonon population and large anti-Stokes shift below 90 K, but the ASPL is still dominated by the phonon-assisted process.

Limited by the available laser wavelengths, we only show the ASPL excited by 780 nm. To find out which laser wavelength is the best to achieve the most efficient phonon-assisted ASPL, we conducted an ASPL excitation (anti-Stokes PLE) measurement, as shown in Figure 3a. The pumping laser wavelengths were tuned from 755 to 790 nm. The ASPL intensity reached a maximum when the photon energy was 50 meV red-detuned below the ZPL. With the photon energy red-detuned further, the ASPL intensity decreased almost exponentially. As discussed previously, the phonon-assisted ASPL intensity follows the phonon population function $[e^{\Delta E/k_B T} - 1]^{-1}$, where no maximum peak exists for any ΔE value. The peak in the anti-Stokes PLE spectra means that there is a resonant mechanism in this ASPL process, where the incident red-detuned photon resonantly absorbs a ∼50 meV phonon and then transits to the ZPL states. Similar resonant-enhanced ASPL has also been reported in laser cooling of CdS, where the longitudinal optical phonon resonantly enhances the phonon-assisted ASPL process and plays an important role in the net cooling observation.[5,19] For diamond, the 50 meV phonon energy is close to the local mode (40 meV) or TA mode (64 meV)[23] shown in Figure 1a. Thus, we propose that the local-mode or TA-mode phonon may involve this resonant up-conversion process.

According to Sheik-Bahae/Epstein (SBE) theory,[3,9] the cooling efficiency $\eta_{cool}(\lambda,T)$ is given by $\eta_{cool}(\lambda,T) = \eta_{exe}\eta_{abs}\lambda/[\bar{\lambda}_{ASPL}(T) - 1]$, where λ is the pump laser wavelength, T is the absolute temperature of the sample, and $\bar{\lambda}_{ASPL}(T)$ is the mean emission frequency. η_{exe} is the external quantum efficiency, and $\eta_{abs} = [1 + \alpha_b/\alpha(\nu,T)]^{-1}$ is the absorption efficiency, quantifying the percentage of photons absorbed that are

DOI: 10.1021/acs.jpclett.8b02862
J. Phys. Chem. Lett. 2018, 9, 6656−6661

engaged in cooling, where α_b is the background absorption coefficient and $\alpha(\nu,T)$ is the semiconductor absorption coefficient. To get net cooling, α_b must be very small and make $\eta_{abs} \approx 1$. In this case, we can estimate the break-even external quantum efficiency to make $\eta_{cool} > 0$. On the basis of Figure 3b, we can estimate that a >97.4% external quantum efficiency is required to achieve net laser cooling for resonant excitation at 759 nm. With more red-detuned pumping at around 780 nm, the breakeven external quantum efficiency of net laser cooling can be reduced to 94.6%, but much higher laser power is needed. Our results show that net laser cooling might be achieved in diamond by improving the external quantum efficiency to higher than 94.6%. Several schemes have been proved to improve the quantum efficiency of SiV and NV emission in diamond, including solid immersion lenses and coupling with the optical cavity. Solid immersion lenses partly inhibit refraction at the surface and enhance the extraction efficiency of photons, where enhancement factors between 8 and 10 can be easily achieved.[28] Another route is to enhance the ZPL emission using the Purcell enhancement effect by coupling the defects with an optical cavity.[29] A 42-fold intensity enhancement has been demonstrated for individual color centers in diamond coupled to monolithic optical cavities, reaching a regime in which spontaneous emission through the ZPL into the cavity mode dominates all other decay channels.

In summary, we have observed anti-Stokes emission of SiV centers in diamond for the first time. By measuring the power and temperature dependences of the ASPL intensities, we confirmed that the ASPL is dominated by phonon-assisted up-conversion via annihilation of phonons. The PLE spectra measurement shows that this up-conversion process can be enhanced by resonantly absorbing a 50 meV TA phonon or local phonon mode. Limited on the low external quantum efficiency in our diamond sample, the net cooling effect has not been observed, but our results show that net laser cooling might be achieved in diamond by improving the external quantum efficiency to higher than 94.6%. Compared with RE-doped materials and semiconductor CdS that has demonstrated a net cooling effect, diamond has high biocompatibility and thus may find potential applications in optical cryotherapy[30] or thermotherapy.[31] By functionalizing the micro- or nanocrysalline diamonds to attach to specific biologically important ligands, optically cooled or heated nanoscopic diamond crystals can destroy diseased or harmful tissues within the body and involve cyclic freezing and thawing of the cells involved. Besides, by combining local light-induced heat or cool sources with sensitive nanoscale diamond thermometry, it may also be possible to engineer biological processes at the subcellular level such as temperature-induced control of gene expression and cell-selective treatment of disease.[32]

METHODS AND EXPERIMENTS

Sample Preparation: The diamond wafer was homoepitaxially grown on a high-pressure and high-temperature Ib diamond substrate by microwave plasma-enhanced chemical vapor deposition. The detailed growth process has been depicted elsewhere.[33,34] Briefly, the precursors used for growth of the diamond are CH_4 and H_2. The pressure in the growth chamber is nearly 330 mbar, and the substrate temperature is nearly 950 °C. After growth, the CVD diamond wafer was removed from the substrate by laser cutting and then used for optical measurements.

Optical Measurements: Stokes PL and ASPL measurements on diamond samples were undertaken in backscattering geometry with a Jobin-Yvon HR800 system equipped with a liquid-nitrogen-cooled charge-coupled detector. The ASPL measurements were undertaken with a 100× objective lens (NA = 0.9) and a 600 lines mm^{-1} grating at room temperature, while a 50× long-working-distance objective lens (NA = 0.5) and 2400 lines mm^{-1} grating were used at low temperature. Excitations of 632.8 and 780 nm were from a He−Ne laser and solid-state laser. A Montana cryostat system was employed to cool the samples down to 4 K from 300 K with a vacuum of 0.4 mTorr. A home-built PLE spectrometer was used for PLE measurements. Monochromatic excitation light was provided by a grating monochromator and an NKT supercontinuum white light source.

AUTHOR INFORMATION

Corresponding Authors

*E-mail: zhangjwill@semi.ac.cn (J.Z.).
*E-mail: cxshan@zzu.edu.cn (C.X.S.).

ORCID

Qing-Hai Tan: 0000-0003-4808-4795
Ping-Heng Tan: 0000-0001-6575-1516
Jun Zhang: 0000-0002-9831-6796

Notes

The authors declare no competing financial interest.

ACKNOWLEDGMENTS

We acknowledge support from the National Basic Research Program of China (Grant Nos. 2017YFA0303401, 2016YFA0301200), NSFC (11574305, 51527901, 11474277, 61604132, and U1604263), and the Strategic Priority Research Program of Chinese Academy of Sciences (Grant No. XDP28000000). J.Z. acknowledges support from the National Young 1000 Talent Plan of China.

REFERENCES

(1) Pringsheim, P. Zwei bemerkungen über den unterschied von lumineszenz und temperaturstrahlung. *Z. Physik* **1929**, *57*, 739−746.
(2) Landau, L. On the thermodynamics of photoluminescence. *J. Phys. Mosc.* **1965**, *10*, 503−506.
(3) Sheik-Bahae, M.; Epstein, R. I. Optical refrigeration. *Nat. Photonics* **2007**, *1*, 693−699.
(4) Seletskiy, D. V.; Epstein, R. I.; Sheik-Bahae, M. Laser cooling in solids: advances and prospects. *Rep. Prog. Phys.* **2016**, *79*, 096401.
(5) Zhang, J.; Li, D. H.; Chen, R. J.; Xiong, Q. H. Laser cooling of a semiconductor by 40 K. *Nature* **2013**, *493*, 504−508.
(6) Disalvo, F. J. Thermoelectric cooling and power generation. *Science* **1999**, *285*, 703−706.
(7) Hehlen, M. P.; Sheikbahae, M.; Epstein, R. I.; Melgaard, S. D.; Seletskiy, D. V. Materials for optical cryocoolers. *J. Mater. Chem. C* **2013**, *1*, 7471−7478.
(8) Nemova, G.; Kashyap, R. A compact integrated planar-waveguide refractive-index sensor based on a corrugated metal grating. *J. Lightwave Technol.* **2007**, *25*, 2244−2250.
(9) Sheik-Bahae, M.; Epstein, R. I. Can laser light cool semiconductors? *Phys. Rev. Lett.* **2004**, *92*, 247403.
(10) Epstein, R. I.; Buchwald, M.; Edwards, B. C.; Gosnell, T. R.; Mungan, C. E. Observation of laser-induced fluorescent cooling of a solid. *Nature* **1995**, *377*, 500−503.

DOI: 10.1021/acs.jpclett.8b02862
J. Phys. Chem. Lett. 2018, 9, 6656−6661

(11) Seletskiy, D. V.; Melgaard, S. D.; Bigotta, S.; Di Lieto, A.; Tonelli, M.; Sheik-Bahae, M. Laser cooling of solids to cryogenic temperatures. *Nat. Photonics* **2010**, *4*, 161−164.
(12) Ha, S. T.; Shen, C.; Zhang, J.; Xiong, Q. H. Laser cooling of organic-inorganic lead halide perovskites. *Nat. Photonics* **2016**, *10*, 115−121.
(13) Li, D. H.; Zhang, J.; Wang, X. J.; Huang, B. L.; Xiong, Q. H. Solid-state semiconductor optical cryocooler based on CdS nanobelts. *Nano Lett.* **2014**, *14*, 4724−4728.
(14) Zaitsev, S. A. M. *Optical properties of diamond*; Springer: Berlin, Heidelberg, Germany, 2001.
(15) Glenn, D. R.; Bucher, D. B.; Lee, J.; Lukin, M. D.; Park, H.; Walsworth, R. L. High-resolution magnetic resonance spectroscopy using a solid-state spin sensor. *Nature* **2018**, *555*, 351−354.
(16) Kern, M.; Jeske, J.; Lau, D. W. M.; Greentree, A. D.; Jelezko, F.; Twamley, J. Optical cryocooling of diamond. *Phys. Rev. B* **2017**, *95*, 235306.
(17) Rose, B. C.; Huang, D.; Zhang, Z. H.; Stevenson, P.; Tyryshkin, A. M.; Sangtawesin, S.; Srinivasan, S.; Loudin, L.; Markham, M. L.; Edmonds, A. M.; et al. Observation of an environmentally insensitive solid-state spin defect in diamond. *Science* **2018**, *361*, 60−63.
(18) Khurgin, J. B. Role of bandtail states in laser cooling of semiconductors. *Phys. Rev. B* **2008**, *77*, 235206.
(19) Khurgin, J. B. Multi-phonon-assisted absorption and emission in semiconductors and its potential for laser refrigeration. *Appl. Phys. Lett.* **2014**, *104*, 221115.
(20) Sun, G.; Chen, R. L.; Ding, Y. J.; Khurgin, J. Upconversion due to optical-phonon-assisted anti-stokes photoluminescence in bulk GaN. *ACS Photonics* **2015**, *2*, 628−632.
(21) Eckhardt, G.; Bortfeld, D. P.; Geller, M. Stimulated emission of stokes and anti-stokes raman lines from diamond, calcite, and α-sulfur single crystals. *Appl. Phys. Lett.* **1963**, *3*, 137−138.
(22) Clark, C. D.; Kanda, H.; Kiflawi, I.; Sittas, G. Silicon defects in diamond. *Phys. Rev. B* **1995**, *51*, 16681−16688.
(23) Feng, T.; Schwartz, B. D. Characteristics and origin of the 1.681 eV luminescence center in chemical-vapor-deposited diamond films. *J. Appl. Phys.* **1993**, *73*, 1415−1425.
(24) Zhang, J.; Zhang, Q.; Wang, X. Z.; Kwek, L. C.; Xiong, Q. H. Resolved-sideband Raman cooling of an optical phonon in semiconductor materials. *Nat. Photonics* **2016**, *10*, 600−605.
(25) Lagomarsino, S.; Gorelli, F.; Santoro, M.; Fabbri, N.; Hajeb, A.; Sciortino, S.; Palla, L.; Czelusniak, C.; Massi, M.; Taccetti, F.; et al. Robust luminescence of the silicon-vacancy center in diamond at high temperatures. *AIP Adv.* **2015**, *5*, 127117.
(26) Morozov, Y. V.; Draguta, S.; Zhang, S. B.; Cadranel, A.; Wang, Y. X.; Janko, B.; Kuno, M. Defect-mediated CdS nanobelt photoluminescence up-conversion. *J. Phys. Chem. C* **2017**, *121*, 16607−16616.
(27) Pant, A.; Smith, B. E.; Crane, M. J.; Zhou, X. Z.; Lim, M. B.; Frazier, S. A.; Davis, E. J.; Pauzauskie, P. J. Optomechanical thermometry of nanoribbon cantilevers. *J. Phys. Chem. C* **2018**, *122*, 7525−7532.
(28) Hadden, J. P.; Harrison, J. P.; Stanley-Clarke, A. C.; Marseglia, L.; Ho, Y. L. D.; Patton, B. R.; O'Brien, J. L.; Rarity, J. G. Strongly enhanced photon collection from diamond defect centers under microfabricated integrated solid immersion lenses. *Appl. Phys. Lett.* **2010**, *97*, 241901.
(29) Zhang, J. L.; Sun, S.; Burek, M. J.; Dory, C.; Tzeng, Y. K.; Fischer, K. A.; Kelaita, Y.; Lagoudakis, K. G.; Radulaski, M.; Shen, Z. X.; et al. Strongly cavity-enhanced spontaneous emission from silicon-vacancy centers in diamond. *Nano Lett.* **2018**, *18*, 1360−1365.
(30) Gage, A. A.; Baust, J. Mechanisms of tissue injury in cryosurgery. *Cryobiology* **1998**, *37*, 171−186.
(31) Li, H.; Huang, Y.; Zhang, B.; Yang, D. W.; Zhu, X. L.; Li, G. X. A new method to assay protease based on amyloid misfolding: Application to prostate cancer diagnosis using a panel of proteases biomarkers. *Theranostics* **2014**, *4*, 701−707.
(32) Kucsko, G.; Maurer, P. C.; Yao, N. Y.; Kubo, M.; Noh, H. J.; Lo, P. K.; Park, H.; Lukin, M. D. Nanometre-scale thermometry in a living cell. *Nature* **2013**, *500*, 54.
(33) Lin, C. N.; Lu, Y. J.; Yang, X.; Tian, Y. Z.; Gao, C. J.; Sun, J. L.; Dong, L.; Zhong, F.; Hu, W.-D.; Shan, C. X. Diamond-based all-carbon photodetectors for solar-blind imaging. *Adv. Opt. Mater.* **2018**, *6*, 1800068.
(34) Chen, Y.; Lu, Y.; Lin, C.; Tian, Y.; Gao, C.; Dong, L.; Shan, C. X. Self-powered diamond/β-Ga_2O_3 photodetectors for solar-blind imaging. *J. Mater. Chem. C* **2018**, *6*, 5727−5723.

DOI: 10.1021/acs.jpclett.8b02862
J. Phys. Chem. Lett. 2018, 9, 6656−6661